Journal Name

ARTICLE

Nanostructured interfaces for probing and facilitating extracellular electron transfer

Leo (Huan-Hsuan) Hsu, Pu Deng , Yixin Zhang, Han N. Nguyen and Xiaocheng Jiang*

Received 00th January 20xx,
Accepted 00th January 20xx

DOI: 10.1039/x0xx00000x

www.rsc.org/

Extracellular electron transfer (EET) is a process performed by electrochemically active bacteria (EAB) to transport metabolically-generated electrons to external solid-phase acceptors through specific molecular pathways. Naturally bridging biotic and abiotic charge transport systems, EET offers ample opportunities in a wide range of bio-interfacing applications, from renewable energy conversion, resource recovery, to bioelectronics. Full exploration of EET fundamentals and implications demands technologies that could seamlessly interface and interrogate with key components and processes at relevant length scales. In this review, we will discuss the recent development of nanoscale platforms that enabled EET investigation from single-cell to network levels. We will further overview research strategies in utilizing rationally designed and integrated nanomaterials for EET facilitation and efficiency enhancements. In the future, EET components such as C-cytochrome based outer membranes and bacterial nanowires along with their assembled structures present themselves as a whole new category of biosynthetic electroactive materials with genetically encoded functionality and intrinsic biocompatibility, opening up possibilities to revolutionize the way electronic devices communicate with biological systems.

I. Introduction

All essential life-sustaining biological processes, such as photosynthesis and cellular respiration, are achieved through a cascade of electron transfers.[1] In most cases, this enzyme-driven process is accomplished intracellularly through a series of biochemical reactions at molecular length scales. Interestingly, certain microorganisms – usually referred as electrochemically active bacteria (EAB) - are able to set-up long-range (>100 μm) and long-term stable (years) electrical connections with extracellular electron acceptors.[2] This **e**xtracellular **e**lectron **t**ransfer (EET) process usually occurs under soluble electron acceptor limited conditions, where EABs can perform as catalysts to directly transfer their respiratory electrons across outer membranes to external solid-state electron acceptors. EET stands out as a unique model system as it breaks the biotic-abiotic boundary to achieve direct energy conversion from biochemical to electrical forms, thus demonstrating potentials in various applications, including energy harvesting,[3] resource recovery,[4] and materials synthesis.[5] Moreover, deeper understanding of EET can reveal the fundaments of biological electron transfer processes, which are extremely valuable for both life sciences studies as well as technological advancements in interdisciplinary research fields, such as the brain–machine interface[6,7] that require communication between biological systems and electronic components. However, the underlying principles of EET are still vague and under active debate due to limitations posed by conventional strategies in interfacing and interrogating EET at relevant length scales. To tackle these challenges, current advances in nanotechnology have opened up opportunities that allow researchers to rationally control and modulate EET pathways to unambiguously determine the key mechanisms and limits and ultimately improve EET efficiency.[8] In this review, firstly, we will discuss the state-of-the-art studies of EET's mechanisms, its implications, and several obstacles faced by researchers in the fields. Secondly, contributions of nanotechnology to EET investigations are introduced in which EET can be precisely probed down to single-bacterium level, thus identifying the key limiting factors in current applications. Lastly, we summarize recent progress in the design and integration of functional nanomaterials to facilitate EET, which holds the potential to inspire novel approaches to further optimize the coupling of biotic EET pathway with abiotic electrodes and broaden various EET's applications.

II. EET: Mechanisms and Implications

A. EET Mechanisms

In the last decades, much effort has been put into investigating EET mechanisms, which have been shown to occur via both indirect and direct routes.[2] In the indirect EET process, EABs secrete small redox-active molecules, such as phenazines,[9] flavins,[10] and quinones,[11] to facilitate the transfer of metabolically-generated electrons to extracellular acceptors. In ideal conditions, these molecules can re-enter the bacteria's bodies and repeatedly aid the electron transfer process; hence, they are commonly referred to as "electron shuttles." Besides indirect EET, EABs are also capable of directly transferring electrons through their outer membranes by electron tunnelling or performing redox reactions with closely-contacted extracellular electron acceptors. It has been identified that this direct

[a] Department of Biomedical Engineering, Tufts University, Medford, Massachusetts 02155, USA. E-mail: Xiaocheng.Jiang@tufts.edu

† Footnotes relating to the title and/or authors should appear here.
Electronic Supplementary Information (ESI) available: [details of any supplementary information available should be included here]. See DOI: 10.1039/x0xx00000x

EET process is mainly accomplished through a cascade of electron transfer processes carried out by a series of surface redox proteins C type cytochromes (cyts).[12–14] In cases where they need to make contact with further-away electron acceptors, EABs can form various micro- to nano-scale extracellular structures to facilitate long-range EET processes. Recent research has demonstrated that two most common EAB species: *Shewanella* and *Geobacter*, can develop pilus-like structures - usually referred to as bacterial nanowire (BNWs) - to remotely access extracellular electron acceptors.[15–17] Two different EET models have been proposed to elucidate the electron transfer mechanism in BNWs, namely: (i) metallic-like electron transfer and (ii) electron hopping. In metallic-like electron transfer model, electrons are hypothesized to transfer through overlapping π-π orbitals of aromatic amino acids in BNWs, which shares similar mechanisms to synthetic organic conducting polymers.[18] On the other hand, in electron hopping model, electron transfer is completed by a series of redox reactions through closely aligned cyts along BNW, which can be illustrated by the well-understood electron hopping mechanism of redox polymers.[19–22]

Moreover, in order to gain deeper understanding of each individual cyt's function, genetic engineering is performed, allowing for the expression or deletion of certain cyts in biofilm.[12,14,23–27] The EET efficiencies of these mutant biofilms can be evaluated by current generation through a microbial fuel cell setup (introduced in next section) or metal oxide reduction experiments. Besides, cyclic voltammetries are commonly applied to study the EET dynamics of both wild-type EABs and their mutants,[14,28] from which the function of individual cyt in EET can be precisely identified. These works are systematically covered in several reviews.[25,26] To summarize, in *Geobacter*, metabolically-generated electrons are transferred from the cytoplasm to outer membrane by periplasmic cyts (e.g. PpcA).[14] Then, outer membrane-to-electron acceptor EETs are mainly facilitated by outer membrane c-type cytochrome Z (OmcZ) and *Geobacter* BNWs (also known as Type-IV pili). These EET processes are also supported by other OMCs (e.g. OmcB, OmcE, and OmcS).[14] In *Shewanella*, the cross-membrane electron transport is carried out by CymA (tetrahaem cytochrome c), followed by transfer to external electron acceptors through metal reduction proteins (e.g. MtrA, MtrB and MtrC).[23,25] Self-excreted flavins also play a role in this EET process as electron shuttles.[10] Alternatively, *Shewanella* BNWs are shown to be extensions of the bacteria's outer membrane which allow electrons to hop to remote electron acceptors via the membrane-bound MtrABC–OmcA tetramers.[16]

Electrochemical impedance spectroscopy (EIS) is another useful tool to quantitatively investigate EET, which is capable of differentiating the charge transfer resistances of biofilm and the contact resistances between biofilms and electrodes.[29] These studies show that the electrical contact at biofilm/electrode interface can be effectively improved by replacing the metal electrode with carbon-based materials as well as increasing electrode surface area. During biofilm development, the charge transfer resistances naturally decrease as a result of the involvement of additional EET pathways.

B. EET Implications

Capable of catalysing both electrical and chemical energy conversions, EET piques growing interest in its implications. Energy harvesting is the most well-developed application of EET, which can be achieved by incorporating EABs in the anode of fuel cells to harvest electrons from their metabolic activities.[30,31] The EET-based device used for harvesting energy is called "microbial fuel cell" (MFC). MFC is proposed as an attractive renewable energy source because of its ability to convert organic waste into electricity, which has demonstrated promising performance in wastewater treatments. Additionally, MFCs can also be configured as biosensors to detect aquatic toxic compounds and monitor water quality.[32] These MFC-based biosensors are commonly employed in wastewater treatment plants to detect the presence of high concentration organic contaminations or toxic compounds (e.g. heavy metals or pesticides). Different types of MFCs along with their working principles have been extensively investigated in the last decades.[3,30,31,33–35] However, most of these studies have suggested that the low power density due to low EET efficiency remains the major challenge to be solved before MFCs could be utilized as reliable power sources or biosensors.

Aside from electricity generation, electrons diverted from EABs can also reduce certain metal ions or soluble organic compounds in wastewater for resource recovery. For instance, MFCs have been used to recover biofuels (methane and hydrogen), nutrients (ammonia and phosphate), and heavy metal ions (e.g. copper, lead, cadmium, zinc, nickel).[4,31] However, the real-world application of this technology is restricted by its high cost and technical difficulty for recovery from rarely concentrated sources. Improving the EET efficiency to enhance the recovery performance is considered as the key to overcome these limitations.

In addition, EET is recently gaining increasing recognition for its potential applications in bioelectronics field. In particular, the protein-based, biosynthetic EET components are being exploited as conductive building blocks for next-generation bioelectronic devices such as biosensors, bio-transistors, and bio-capacitors.[5,36] The nontoxic, room temperature, and water-based production of these genetically encoded, electroactive biomaterials differs substantially from that of traditional synthesis/fabrication strategies. More importantly, they provide the unique potential to mediate the intrinsic biophysical and biochemical mismatches between biological systems and artificial electronics for a range of bio-interfacing applications including biomedical sensing, prosthetics, and bio-computation. However, compared with conventional electronic materials such as metals, semiconductors and conductive polymers, the conductivities of these biosynthetic materials are significantly lower, thus improving their electrical properties would be critical for their eventual utilization in bioelectronic applications.[34]

In short, EET has demonstrated outstanding potentials in many fields, including energy generation, resource recovery, and bioelectronics. However, EET's low efficiency remains a major challenge that hinders the developments of its applications, thus presenting an urgent need for researchers to better understand the fundamental mechanisms of EET so as to identify and address the key limiting factors. Therefore, tools that could seamlessly interface with EET at relevant length scales are highly demanded. The emerging nano- and micro-technology can be very unique in probing and controlling the molecular- through cellular-level processes. In next section, we will critically review the recent progresses in the design and application of these small-scale tools for EET studies that have yielded biological insights that would have been inaccessible through traditional population-level experiments.

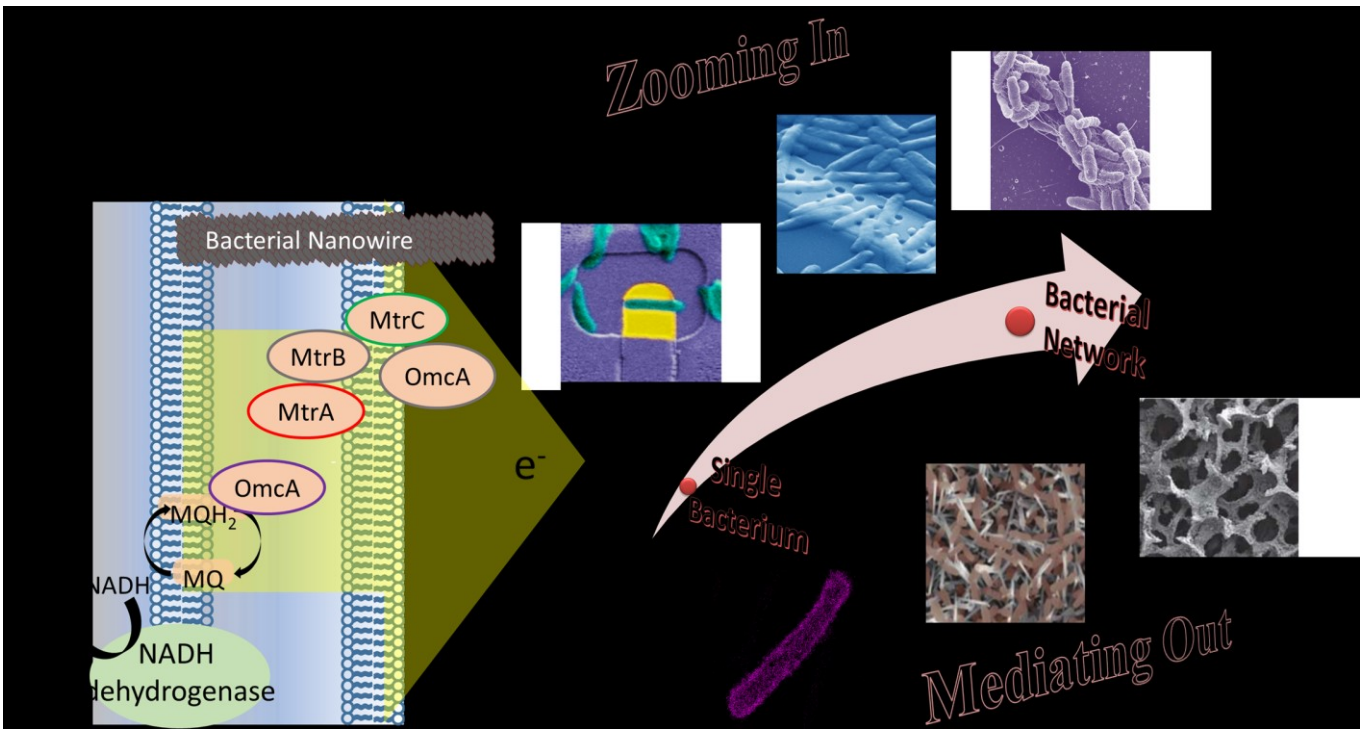

Fig. 1 Scheme of nanotechnology enabled EET based mechanism studies and efficiency elevations in a rationally-designed, synthetic ecosystem across different length scales: from single bacterium current generation, to bacterial-electrode interaction, and eventually to bacteria-bacteria EET and network level. Reprinted with permission from ref. 45, 69 (Copyright 2018, Wiley-VCH), 81 (Copyright 2014 American Chemical Society), 87 (Copyright 2018 American Chemical Society), 91 (Reproduced permission from The Royal Society of Chemistry).

III. Nanotechnology Enabled EET Investigation

In native biofilm, EABs' cellular materials (e.g. cytoplasm, outer membrane etc.) and their self-assembled electroactive components in extracellular polymeric substances (EPS) serve as basic building blocks to construct various electron transfer pathways for long-range EET. Most of these EET components demonstrate conductivities in the range 10^{-9} S·cm^{-1} to 10^{3} S·cm^{-1}.[34] Outer membranes play a key role in transferring intracellular metabolic electrons to terminal electron acceptors, and could also function as intermediate conduits in long-range charge transport. Outer membranes of *Shewanella* and *Geobacter* are mainly consisted of cyts that have been systematically studied and summarized in Section II. Nevertheless, the comprehensive understanding of extracellular charge transport is still limited by the complexity of EPS that contains proteins, nucleic acids, humic substances, lipids, and BNWs. Many efforts have been made to investigate the functions of each components in the EET processes. In particular, different types of BNWs have been found to be directly associated with biofilm conductivities[37]. Scanning tunnelling microscopy[15] and conducting-probe atomic force microscopy[17] have been utilized to characterize the electrical properties of these nanoscale materials. By scanning BNWs isolated from EABs under desired bias voltage against pyrolytic graphite substrate, researchers demonstrate the conductive nature of both *Shewanella* and *Geobacter*'s BNWs for the first time. In later studies, the conductivities along these BNWs are investigated via two-terminal current-voltage measurements with fabricated nanoelectrodes. Based on these measurements, the conductivity of *Shewanella*'s BNWs is determined to be in the range of 60 (mS·cm^{-1}) to 1 (S·cm^{-1}),[38] whereas that of *Geobacter*'s BNWs is within 51±11 (mS·cm^{-1}).[39] These measurements strongly indicate that BNWs are not the only factors determining the overall EET efficiencies since their conductivity is sufficient to discharge the entire electrons generated from metabolism of a single EAB (10^{6} electrons per cell per second) to electron acceptors.

While these ex-situ, "top-down" strategies have provided important insights about charge transport within isolated, fixed EET "modules," the ultimate understanding of EET needs to be placed in the context of relevant microenvironment where EET occurs. When the local pH increases from 2.7 to 10.5, for instance, *Geobacter*'s BNWs' conductivity decreases from 188±34 (mS·cm^{-1}) to 37±15 (mS·cm^{-1}).[39] A "bottom-up" paradigm is recently emerging, where nanotechnology-enabled platforms are being developed to rationally engineer and probe individual cells, their local environments and cellular interactions to provide more comprehensive and biologically relevant information about native EET. Different from the aforementioned top-down approaches, it represents a unique strategy to precisely interpret and interrogate key steps of the entire EET process in a rationally-designed, synthetic ecosystem: from single bacterium current generation, to bacterial-electrode interaction, and eventually to bacteria-bacteria EET and network level performance (Fig. 1). From these studies, a sophisticated EET model can be built to comprehensively illustrate the cascade of electron transfer processes. Currently, these approaches have provided unambiguous insights into single bacterium's EET efficiency

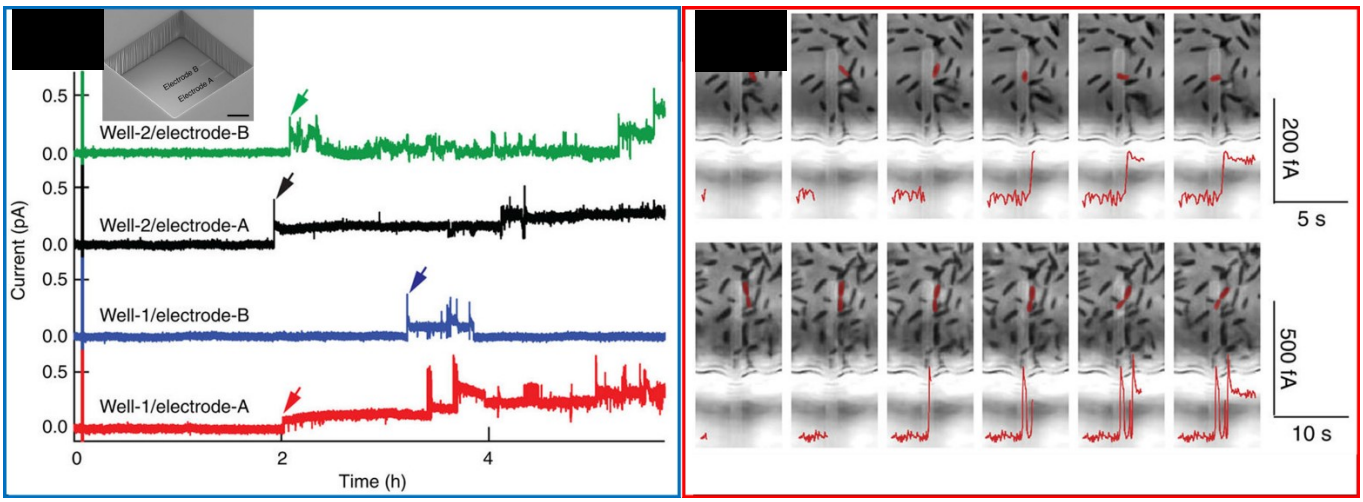

Fig. 2 Multiplex electrochemical measurements of *Geobacter sulfurreducens* DL-1 at single bacterium level.[42] (a) EET current recording on four selected electrodes in two isolated wells. Recording is started immediately after bacteria introduction; the red, blue, black and green arrows mark the occurrence of the first current step on each electrode at ~1 h after inoculation; inset: SEM image of a pair microelectrodes in microwell for EET current recording and (b) Evolution of in situ phase-contrast images of DL-1 cells on and around the measured electrode when a 82-fA (one bacterium contact) (top) and 185-fA (multi-bacteria contact) (bottom) current spike is recorded, respectively. Reprinted with permission from ref. 42.

and also revealed key factors in bacterium-electrode and bacterium-bacterium interactions that play critical roles in determining the overall EET efficiency.

A. Single cell measurement

The heterogeneity of biofilm introduces numerous variations in the populational level studies of the bacterial behaviours which can be overcome by precisely probing cellular dynamics at single bacterium level.[40,41] In the context of EET, probing the electrochemistry at single EAB level with precisely modulated microenvironments and bacterium-electrode contacts can help unravel the heterogeneity and complexity in biofilm-level measurement, thus unambiguously determining the fundamental limits and mechanisms of EET. Micro-/nano-fabricated electrodes, with dimension comparable to individual EABs, have been demonstrated as powerful tools to analyse cross-membrane EET at single-bacterium level. Jiang et al. report the first single-bacterium level electrochemical study of *Geobacter sulfurreducens* DL-1 using optically transparent microelectrode arrays confined in separated microchambers.[42] (Fig. 2 (a) insert) This device allows localized current recordings from multiple electrodes within a controlled microenvironment. Measurements are initiated by injecting DL-1 into the device. Two hours after the injection, all recorded currents of four electrodes (in two separated wells) show stepwise increases (Fig. 2 (a)). Each current increase consists of two processes: an initiation by a fast decaying peak attributed to the quick discharge from the cell membrane with accumulated electrons, followed by a stable plateau corresponding to sustained cross-membrane EET from DL-1. The multiplex recordings suggest that these current increases are localized to individual electrodes and directly associated with the bacteria-electrode contacts. This conclusion is supported by the simultaneous electrical recording and optical imaging, which demonstrate that the recorded current increased to ~ 82 fA (Fig. 2 (b) top) immediately after single DL-1 makes a physical contact with the electrode surface. Furthermore, the contact of a two-bacterium assembly with measured electrode leads to a larger current increase of ~ 185 fA (Fig. 2 (b) bottom), showing that the current amplitude is determined by the number of DL-1s that are involved in the interaction. Besides, the long range direct EET can also be detected by this platform. As presented in the long-term measurements, a dramatic rise (more than 5 folds) of recorded current is observed when a close packed network is formed. It is noteworthy that the change in bacterial number on measured electrodes (7-to-10 and 6-to-8) is negligible compared with the magnitude of current increasing. These results indicate that this dramatic current increase does not only originate from direct bacteria–electrode interactions but also from the surface protein and/or BNW-enabled long-range EET in the developed DL-1 network.

Compared with *Geobacter* which has only been associated with direct EET mechanisms, *Shewanella* can perform both direct and indirect cross membrane EETs, making the investigations more complicated. Liu et al. develop a platform that combines an optical tweezer and a micropatterned ITO electrode to access the EET current generated by single *Shewanella loihica* PV-4, where the current generation can be studied in the context of single cell/electrode interaction and constant electron mediator background.[43] In particular, motions of single PV-4 can be manipulated by an optical tweezer generated by focusing a Nd:YAG laser (2 mW, wavelength = 1064 nm) through a 100 X oil-immersion objective lens. By moving the objective lens vertically, the optically trapped PV-4 can be attached to and detached from the ITO electrode (Fig. 3 (a)). The electrochemical current between PV-4 and ITO (poised at 0.2V) is continuously measured under strict anaerobic conditions to eliminate the influence from O_2. During the measurement, the stable background current can be recorded when PV-4 is detached from ITO. Moving PV-4 to physically contact the ITO electrode leads to a rapid increase in the measured current (Fig. 3

(b)). This current is stabilized at certain point during PV-4-electrode contact, which is attributed to the constant respiratory electron output from PV-4. After detaching PV-4 from the ITO electrodes, the measured current immediately reduces to its background level. The EET current of single PV-4 can thus be calculated at approximately 200 fA by subtracting the background current from the current recorded during PV-4-electrode contact (Fig. 3 (b) top). In a separate measurement, PV-4 with reduced amount of surface cyts cannot generate similar response (Fig. 3 (b) bottom), which further demonstrates that the current increase during PV-4 attachment is originating from the surface protein mediated direct EET.

These single-bacterium measurements also enable the estimation of the intrinsic limit of MFC current density, which could be calculated by dividing single DL-1 or PV-4 current outputs by the physical volume of EAB. This estimation gives a value of 10^6 (A/m^3) which is 2–3 orders of magnitude higher than the best volumetric current density reported in working MFCs.[44] This estimation indicates that the low performance of most EET implications is not restricted by the cross membrane EET efficiencies of EABs but rather by other factors including longer range charge/mass transport at network levels.

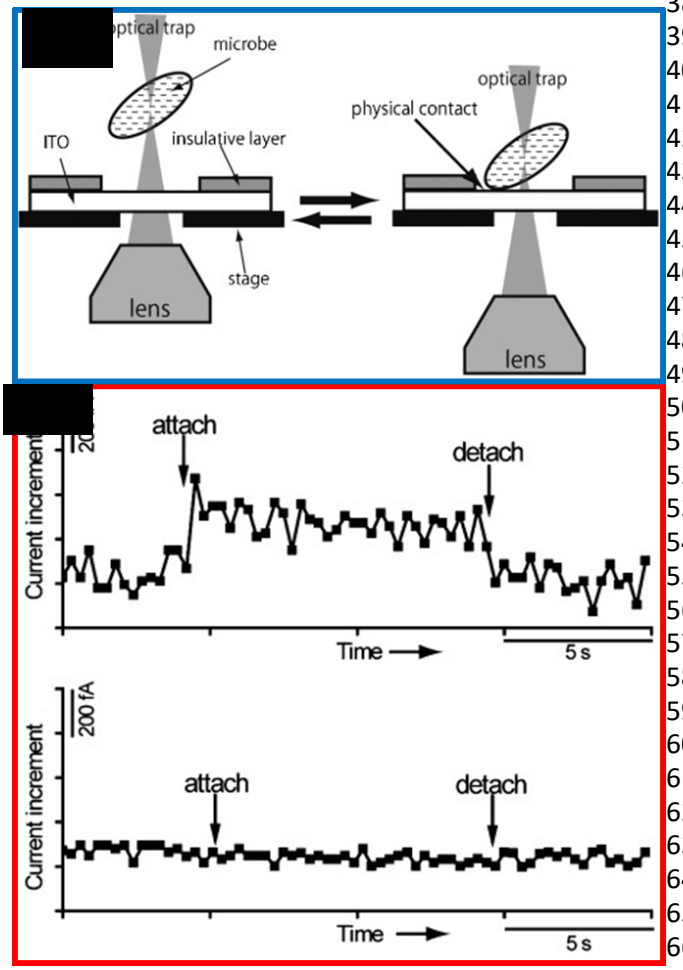

Fig. 3 Single *Shewanella loihica* PV-4 measurement. (a) Schematic of EET measurement platform with incorporated optical tweezer and microelectrode; and (b) short circuit current measurements when (b1) wild type PV-4 and (b2) PV-4 with reduced amount of surface cyts attached to and detached from microelectrodes. Reprinted with permission from ref. 43. Copyright 2010, Wiley-VCH

EABs can interact with electrodes through both direct (physical contact) and indirect (mediator) EETs. A detailed understanding of EAB-electrode interactions and how these processes are translated into current generation can provide important insights on improving EET efficiency at this heterogeneous interface; however, the limitations posed by conventional EET measurement techniques still challenge the deconvolution of these mechanisms. To address these challenges and better understand the fundamental electron transfer mechanisms between EABs and electrodes, Jiang et al. have developed a nanoscale measurement platform which allows accurate control of physical contacts between individual bacterium and electrodes,[45] enabling unambiguous differentiation between these two mechanisms. This platform consists of two types of nanostructured electrodes covered by a silicon nitride passivation layer. To regulate the EAB/electrode contact, this silicon nitride layer is patterned by e-beam lithography and reactive ion etching to comprise either 150 nanohole (200 nm × 400 nm) array or single micro-window (6 µm × 10 µm) openings (Fig. 4 (a)). Both *S. oneidensis* MR-1 and *G. sulfurreducens* DL-1, two model EAB systems, have been studied using this platform. As presented in the SEM images (Fig. 4 (b)), during the measurement, bacteria on the nanoholes are prohibited from direct physical contact with the electrode; therefore, electrons can only be transferred by diffusible mediators. Alternatively, both mediators and surface cyts can contribute to the EET processes of bacteria which are in contact with micro-window electrodes. Short-circuit current (vs. Ag/AgCl reference) on both types of electrodes is recorded to quantitatively differentiate the contribution of direct EET mechanism from that of mediated EET mechanism. During *S. oneidensis* MR-1 measurement, both nanohole and micro-window electrodes reach a steady state current of 5 pA within 15 min after inoculation. The in-situ phase-contrast imaging confirms that MR-1 cells do not develop contacts with either electrode within this short time frame. Moreover, both recorded currents stay constant during 50 min recording period, despite the increasing amounts of bacteria that are in contact with micro-window electrode after 20 min incubation (Fig. 4 (c)). These observations suggest that physical contacts between bacteria and electrode are not essential in early stage EET of MR-1. In longer term short-circuit current measurement after biofilm formation, micro-window electrode still records similar level of current as nanohole electrode. Furthermore, both electrodes respond similarly to the removal and re-introduction of mediators which lead to 95% reduction and 80% recovery of EET currents, respectively. These results indicate that mediator-driven indirect EET plays the major role in EET of MR-1. As a comparison, in the long-term measurement of *Geobacter* DL-1, current generation can only be observed on the micro-window electrode within the first 8h, indicating the electron transfer of DL-1 is dominated by the direct EET at the initial stage (Fig.4 (d)). Overall, this nanotechnology-based platform consisting of engineered nanoelectrodes and in situ optical imaging represents a

unique tool to unambiguously address the fundamental mechanism of EET in the context of EAB-electrode interactions.

B. EET Study at Network Level

Native EAB biofilms grown on solid-phase electron acceptors, such as MFC anodes, are usually tens of micrometers in thickness. As a result, the majority of bacteria have to perform long range EET to remotely "dump" the respiratory electrons and complete the metabolic cycle. Hence, a better understanding of inter-cellular EET is ultimately central to understanding the performance of bioelectrochemical systems at ensemble level. Furthermore, this knowledge can create the possibilities to manipulate the EET process for applications beyond energy harvesting (e.g. bioelectronics and biocomputing). Technically network-level EET investigation has been mainly challenged by the intrinsic complexity of native biofilm which contains a heterogeneous mixture of EABs and EPS components (such BNWs, polysaccharides, humic substances etc.) with a broad spectrum of electrical properties.[34] The recent development and application of nano- and micro-technology has opened up new possibilities to overcome these challenges, in which the cellular interaction, microenvironment and local electrochemistry can be rationally controlled to precisely construct and interrogate EET pathways at a range of length scales.

Malvankar et al. design a platform which contains a pair of gold electrodes separated by a non-conductive gap of 50 µm bridged by a confluent *Geobacter sulfurreducens* DL-1 biofilm. This platform allows for specific measurement of the long-range EET of DL-1 in-situ.[19] Through (1) controlling the culturing conditions to regulate the development of conductive pili; as well as (2) applying the genetic engineering tool to suppress the expression of all outer membrane cytochromes, this platform demonstrates that the conductive pili are the most essential component to electrically bridge *Geobacter* for long range EET. Combing the results from temperature-dependent conductivity measurement, Malvankar et al. propose a "metallic-like" EET mechanism of *Geobacter* network that the electrons are delocalized and move through the π-conjugated aromatics across the bacterial network.

Alternately, Snider et al. study the long-range EET within *Geobacter sulfurreducens DL-1* biofilm grown on an interdigitated microelectrode array (IDA). This IDA contains 2 interdigitated electrodes (electrode 1 and 2, each comprised of 50 microelectrode bands) with 15 µm separations between adjacent pair.[46] After biofilm growth under biased potential at 0.300 V (vs. Ag/AgCl), two types of electrochemical studies are performed. In the first type, the potential applied to electrode 1 is swept from 0.300 V to -0.750 V which continuously performs as the only EET terminal to accept the electron generated by acetate oxidation on the biofilm. Simultaneously, the open circuit potential of electrode 2 is measured, which indicates the oxidation state of the biofilm. In the second type, potentials of both electrode 1 and 2 changes during measurement while maintaining a constant (0.1 V) potential difference. This potential difference establishes an EET pathway across the 15 µm biofilm between each adjacent electrode pair in which one electrode with a relatively positive potential acts as electron source, while the other one acts as electron drain. Notably, the potentials of both electrodes are controlled in the range that no acetate oxidation can be triggered; therefore, the electron transfer event can only occur in the biofilm between two electrodes. The results of both type 1 and 2 measurements fit well with the multistep electron hopping numerical model. The model suggests that the redox gradients of biofilm are present in the vicinity of each

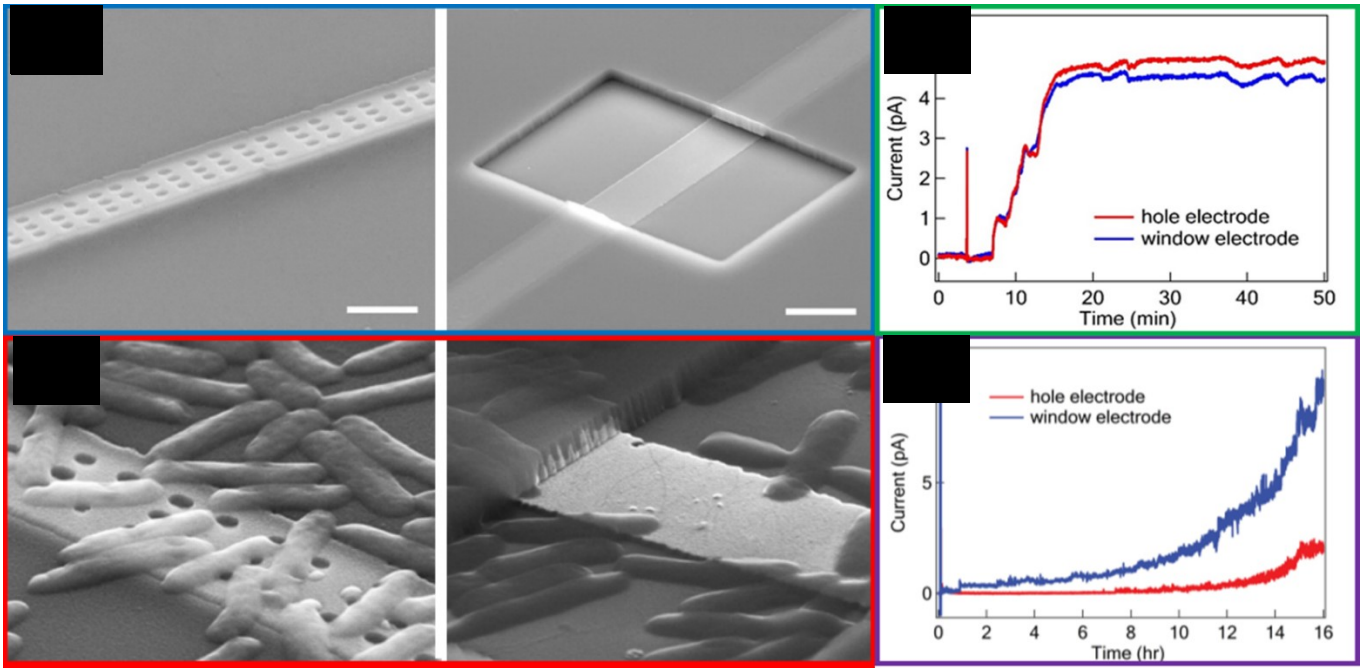

Fig. 4 Nanostructured electrodes for probing EET. (a) SEM images of nanohole and micro-window electrodes; (b) SEM images of MR-1 on nanohole and micro-window electrodes at ~1 h after inoculation; and long term EET current measurements of (c) MR-1 and (d) DL-1 on both nanohole and micro-window electrodes.[45]. Reprinted with permission from ref. 45.

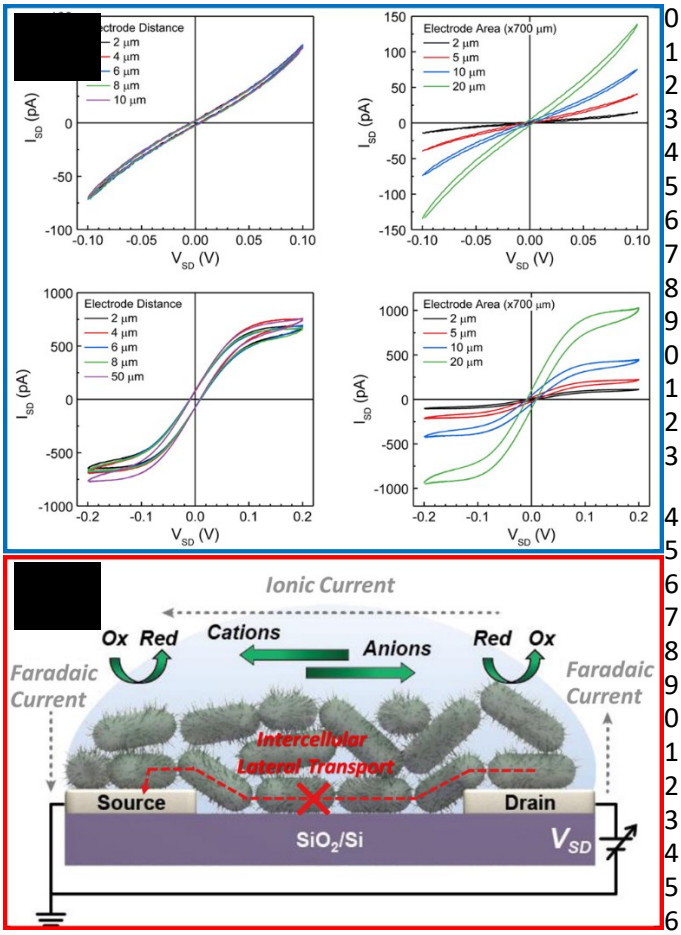

Fig. 5 On-chip nanoelectronic investigation of EET. (a) two terminal I-V measurements of *Shewanella oneidensis MR-1* and *Geobacter sulfurreducens PCA* on microelectrode arrays with different electrode areas and electrode distances; and (b) schematic of the electrochemical-reaction dominated EET mechanism proposed by Ding et al. Reprinted with permission from ref. 47. Copyright 2016 American Chemical Society

electrode during both measurements. This redox gradient can drive electrons transport either from acetate oxidation on biofilm to electrode 1 (type 1) or between two electrodes (type 2). Based on these results, Snider et al. propose a multi-site electron hopping mechanism that the EET of DL-1 network is driven by the redox gradient between electron donors and acceptors.

Moreover, Ding et al study the EET mechanisms in both *Shewanella oneidensis MR-1* and *Geobacter sulfurreducens PCA* networks using a customized microelectrode array which contains paired microelectrodes with various surface areas and separations.[47] In two terminal current-voltage measurement with the applied potential from – 0.2 V to 0.2 V, the response currents across both EABs are independent of the electrode separations but strongly correlated with the electrode areas (Fig. 5 (a)), thus suggesting that the measured EET is dominated by the electrochemical reactions at the bacteria-electrode interfaces. To independently detect the electrochemical (from EABs to counter electrode) and electron transfer (across EAB bridged pair electrodes) components of this system, electrical transport spectroscopy (ETS) is carried out on MR-1 biofilm as a model system. In the ETS studies, the counter electrode functions as a gate electrode (similar to the conventional field effect transistors), and the reference electrode (Ag/AgCl) is used to regulate the electrical potential applied on the EABs. The measured electrochemical currents and the electron transfer currents exhibit comparable amplitudes which indicate that the measured electron transfer process is closely correlated with electrochemical reactions. Based on these results, Ding et al. introduce an alternative model to explicate the EET mechanisms (Fig. 5 (b)) that the electron transfer is determined by the electrochemical reactions at the bacteria-electrode interface. In this model, the direct electron transfers across biofilms does not exist; whereas, the EET is completed by coupling the electrochemical reactions at both terminals of biofilms though liquid phase ionic charge transfer.

Overall these customized microelectrode platform enables electron transfer measurement with controlled electrochemistry and bacteria-electrode interactions. The discrepancy between their conclusions, however, indicates the intricacy of long-range EET mechanisms which could be further complicated by the heterogeneity of EAB biofilms. Hence, there is a strong need to further optimize these EET studies by establishing a rationally designed bacterial network where microenvironments and bacterium-bacterium interactions can be precisely manipulated. This effort can potentially lead to a full understanding of structure-function correlation in the context of bacterial interactions to unambiguously elucidate the underlying EET mechanisms in the bacterial networks.

IV. Nanostructured Materials for Facilitating EET

EET performed by electrochemically active bacteria, though holding tremendous potentials, still has limited efficiency. This challenge posed by the natural EET process is hindering most downstream applications such as energy conversion and resource recovery. For example, a combination of hydrodynamic experiments and numerical modelling of the response of *G. sulfurreducens* biofilms cultured on a rotating disk electrode demonstrate that the cells furthest from the electrode are limited by the rate at which electrons could be transported through the extracellular matrix and are determined to be respiring close to their basal metabolic rate.[48]

Nanoscale materials, such as metal/semiconductor nanoparticles and carbon nanotubes, have been extensively studied to promote electron transfer in bioelectrocatalysis.[49] The electron transfer rate in amperometric biosensors or enzymatic fuel cells, for example, has been found to be significantly improved by incorporating nanostructures that allow for optimal alignment of bioelectrocatalysts and thus more effective coupling with active redox centres.[50–53] For EABs, the whole bacterium, instead of individual biomolecules, is involved in biocatalytic process; nonetheless the charge transport is fundamentally carried out through EET-specific molecules/molecular assemblies thus could also benefit from similar approaches. In this part, we will present and critically discuss the research strategies that have been developed to

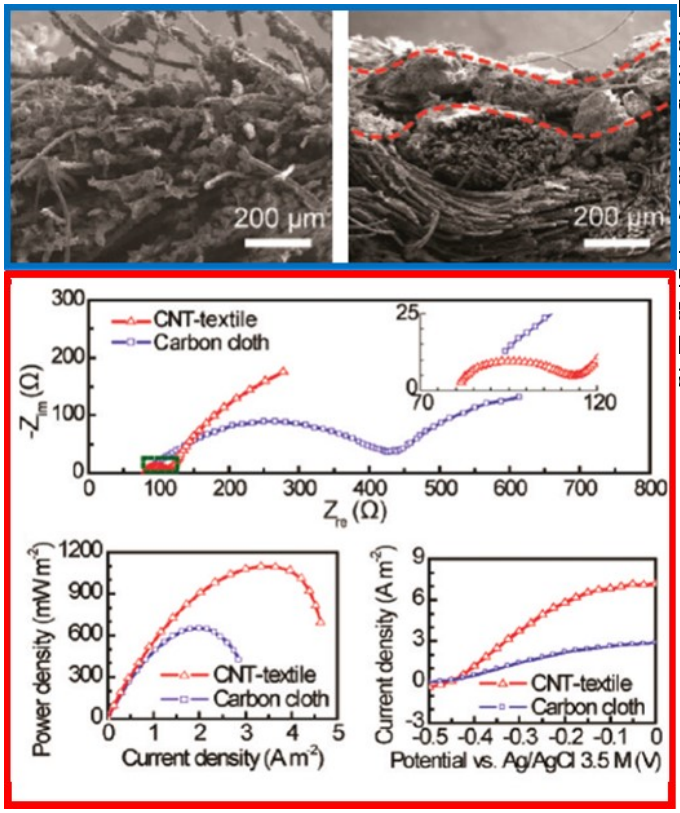

Fig. 6 CNT-textile anode enabled MFC performance improvement. (a) SEM images of the bacteria growth on the CNT-textile (left) and the carbon cloth (right) anodes and (b) Performance of MFCs equipped with CNT-textile and carbon cloth anodes. Reprinted with permission from ref. 54 Copyright 2011 American Chemical Society

utilize rationally designed and integrated nanomaterials for EET facilitation at both EAB/electrode and EAB/EAB interfaces.

A. Facilitating EET at EAB/Electrode Interface

As the terminal electron acceptors for many EET applications, electrodes, particularly their interfaces with EABs, are playing critical roles in determining the overall device performance. However, several intrinsic mismatches in biophysical/biochemical properties between bacteria and conventional electrode materials restrict the EET efficiency at these biotic-abiotic interfaces. With rationally designed structure and physical/chemical properties, bottom-up synthesized nanomaterials hold great promise for overcoming this barrier. Below we will discuss several strategies that have been exploited for electrode modification to facilitate the electron exchange with EABs.

Traditional MFC electrodes (mostly carbon-based) usually involve designs that feature increased surface area (e.g. carbon cloth, graphite brush, stainless steel brush, carbon paper etc.) to reduce the contact impedance with EABs. Recently Xie et al. have developed a porous, hierarchically structured anode comprising wined polyester fibers with conformally coated CNTs to further improve the power extraction.[54] In this anode, macro-pores provide 3D openings which allow bacteria to form biofilm inside the space. In comparison with traditional 2-D electrode, the biofilm developed on this CNT-textile 3-D scaffold features 10-folds improvement in the ion-biofilm-anode interfacial area for better mass transport (Fig. 6 (a)). The nanostructured CNT surface also creates additional roughness, providing strong mechanical binding between the developed biofilms and electrodes. These improvements lead to 90% reduction of internal resistance (30 Ω v.s. 300 Ω) and significantly improved power density (1098 vs 655 mW m^{-2}) as compared with 2D electrode (Fig. 6 (b)). Moreover, other studies have also demonstrated that CNT can trigger the structural transformation of OMCs' porphyrin ring on *Shewanella*. The Fe^{2+} redox active centre can thus be more intimately coupled with CNT via electron tunnelling, which leads to a 10-time increase in bioelectrochemical systems' current

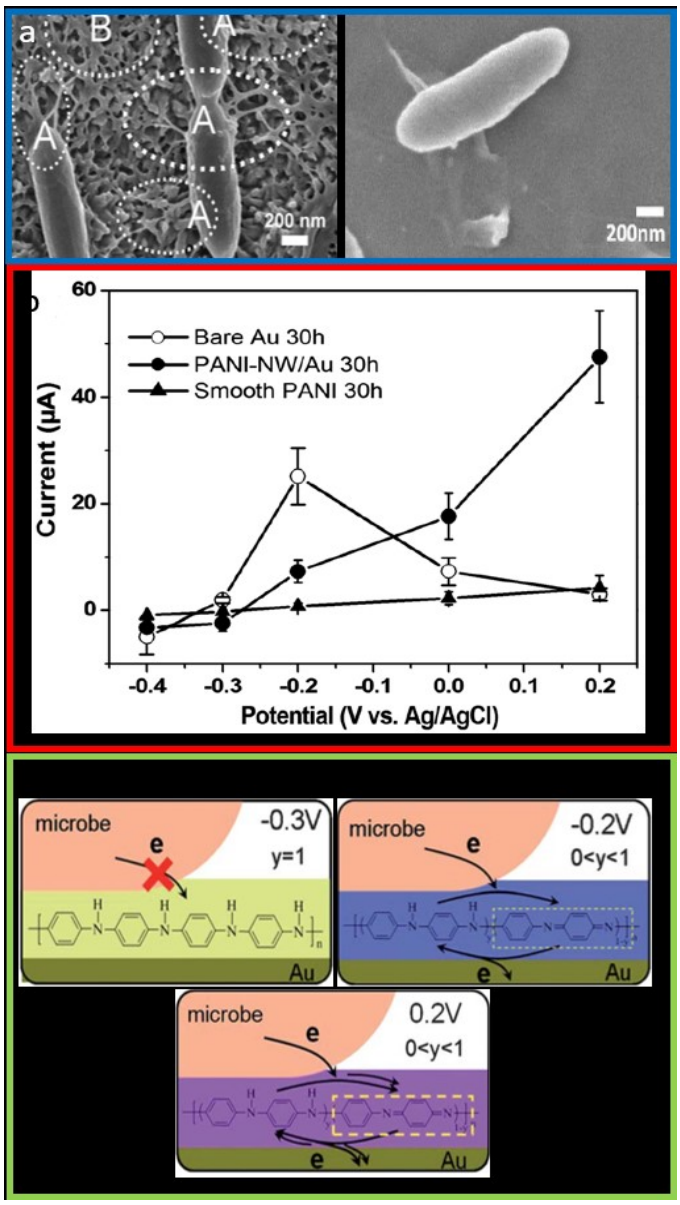

Fig.7 PANI-NA electrode mediated EET. (a) SEM images of cells on a PANI-NA/Au electrode (left) and smooth electrode (right); (b) Influence of poised potentials on EET currents on PANI-NA/Au (solid circles), smooth PANI/Au (solid triangle) and bare Au (open circles) electrodes; (c) Schematic of bacterial EET on a PANI-NA/Au electrode under different poised potentials. Reproduced from Ref. 61 with permission from the Royal Society of Chemistry

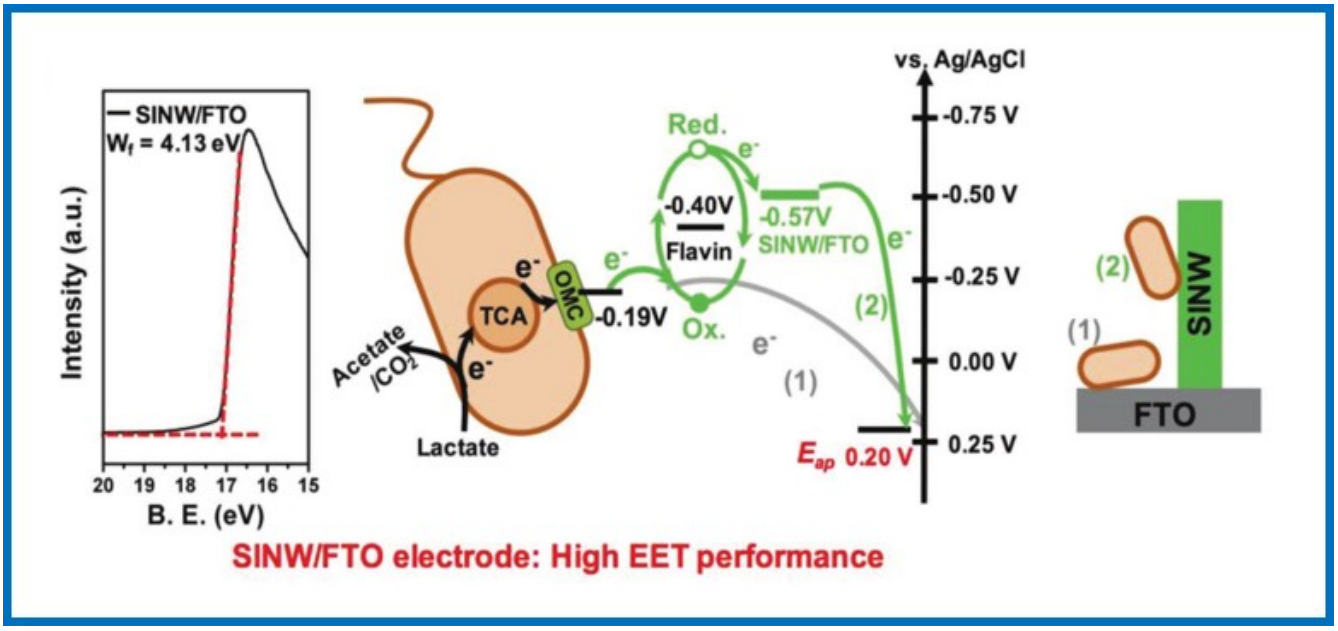

Fig. 8 SINW/FTO electrode for facilitating both direct and indirect bacterial EET. (left) The cut-off energy region of UV photoemission spectroscopy spectrums of SINW/FTO electrode. (Right) Schematic of the cascade of EET across bacteria/FTO interfacing with SINW mediated energy levels. Reprinted with permission from ref. 69. Copyright 2018, Wiley-VCH

generation.[55,56] Similar strategies have also be explored in creating other 3-D macroporous electrodes for various applications.[57–60]

Certain EABs have been known to secrete soluble mediators as electron "shuttles" when direct EET becomes challenging. Inspired by this naturally developed strategy, nanomaterials with multiple redox states have been explored by many groups to modify the electrodes which not only expand the electrode/bacteria contact area but also facilitate EET as solid-state mediators. For example, Ding et al. have generated a vertically-aligned polyaniline nanowire array (PANI-NA) on a gold (Au) electrode.[61] PANI is a conductive polymer which contains alternating oxidized (quinone ring) and reduced (benzene ring) repeat units, and the ratio of these two redox contents could be tuned by externally applied potential. In this electrode design, highly oriented 3D nanostructures of PANI-NA greatly improve bacteria-electrode adhesion through enhanced local topographic interactions (Fig. 7 (a)). Correspondingly, a 51 μA current is recorded on the PANI-NA/Au electrode, which is over 10 and 25 times higher than smooth PANI/Au and bare Au electrode, respectively. In addition, Fig. 7 (b)&(c) show that the bacteria EET currents can be further increased by raising the applied potentials. With the positive shift of external potential, reduced units in PANI polymer chain are converted to oxidized states, which has similar function as flavin to mediate the electron transfer. This work demonstrates the possibility to improve EAB-electrode coupling through (1) promoting the physical/topological contacts and (2) tuning the interfacial redox states to reduce the charge transfer barrier. Similarly, a variety of other nanomaterials have also been explored in the electrode modification to facilitate EET at bacteria/electrode interface such as polypyrrole[62,63], nano-structured Au/Pd,[64,65] TiO_2,[66] MnO_2,[67] and NiO[68] etc.

Besides, the rational design and tuning of materials' electronic properties offers additional possibility to bridge the energy gap at EAB/electrode interface. To engineer the most efficient and compatible electrodes, the selection and modification of nanomaterials are of utmost importance. As an outstanding material candidate for this purpose, nanoscale semiconductors allow for the precise modulation of their electronic states through synthetic control. Based on this strategy, Bian et al. have come up with a platform that incorporates In_2O_3 nanowire arrays on a flat F-doped In_2O_3 (FTO) electrode.[69] The Fermi levels of these In_2O_3 nanowires can be tuned to a desired range by Sn doping to reduce the energy barrier at bacteria-electrode interface. In this work, the Fermi levels of Sn-doped In_2O_3 nanowire (SINW) are set at -0.57 V to match with other electron transfer components, namely FTO (Fermin level = -0.02 V), outer membrane cytochrome (OMC) (Fermi level = -0.2V), and the electron shuttle flavin (Fermi level = -0.4 V). Consequently, under a 0.2 V potential, SINWs can effectively facilitate both direct (OMCs (-0.2V)-to-FTO (-0.02 V)-to-external potential (0.2V)) and indirect (flavin (-0.4V)-to-SINW(-0.57V) -to-external potential (0.2V)) EETs (Fig.8). Introducing additional flavin/malonic acid only effectively enhances/inhibits indirect EET process in the system equipped with SINW/FTO electrodes, which further confirms that the indirect EET is promoted by SINW. Overall, these unique properties of SINWs can lead to a 60 times enhancement in current generation as compared with that of a flat FTO electrode. Based on similar strategies, several other nanomaterials with proper Fermi levels such as α-Fe_2O_3, goethite, and Fe_3O_4 have also been exploited as materials suitable to modify electrode's properties to match bacteria OMCs' energy level and close the charge transfer gap.[70–72]

Moreover, aforementioned strategies can be further modified to incorporate photosensitive nanoscale semiconductors to achieve

optically-regulated EET. Qian et al. have developed a α-Fe_2O_3 nanowire-based anode to enable photo-enhanced electrochemical interactions between α-Fe_2O_3 and bacteria.[73] Specifically, under light illumination, α-Fe_2O_3 nanowires generate photoexcited electron−hole pairs. The photogenerated holes in the valence band accept electrons from *Shewanella*, while the photogenerated electrons flow through an external circuit for cathodic reduction (Fig. 9). This effect results in a 150% increase in current density as compared with the two other control setups which contain either dead- or no bacteria on the α-Fe_2O_3 anodes. Qian et al. suggest that the current enhancement is attributed to the additional redox species associated with MR-1 cells that are thermodynamically favourable to be oxidized by the photogenerated holes. In contrast, without illuminations, all three anodes (live bacteria, dead bacteria, and no bacteria) cannot generate current. These results indicate that light can regulate the EET process by turning on and off certain EET pathways between *Shewanella* and α-Fe_2O_3.

In addition, nanomaterials are also applied to facilitate resource recovery through enhanced electrosynthesis (reversed EET). For example, Nie et al.[74] introduce nickel (Ni) nanowires as the interfacing layer between *Sporomusa* biofilm and graphite electrode. The Ni nanowire network provides sufficient surface roughness and porosity to accommodate *Sporomusa* biofilm with higher cell density than that of the bare graphite electrode. In combination with the significantly increased electroactive surface area, the new electrode design leads to a 2.3 fold increase in bio-reduction rate of carbon dioxide for acetate generation and 82.14% of the electrons consumed are recovered in acetate. Similarly, gold, palladium, or nickel nanoparticles are also applied by Zhang et al. to assist the electrosynthesis process of Sporomusa, resulting in 6, 4.7 and 4.5 fold increase in electrosynthesis rate as compared with that of the untreated carbon cloth electrode, respectively.[75]

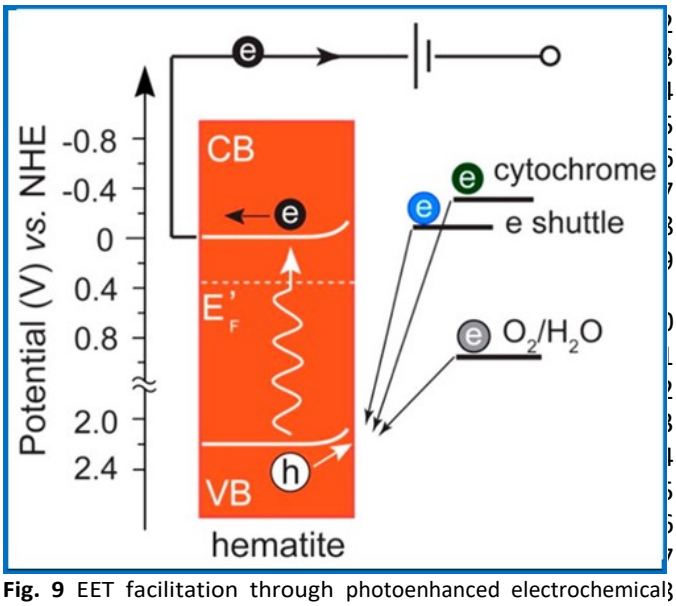

Fig. 9 EET facilitation through photoenhanced electrochemical interactions between hematites and bacteria. Energy diagram of the α-Fe_2O_3 (hematite) photoanode in the MPS. Reprinted with permission from ref. 73. Copyright 2010 American Chemical Society

B. Facilitating EET at Network Level

Electrode modification with functional nanomaterials represents an effective approach to facilitate EET at EAB/electrode interface. To improve the overall EET efficiency at network level, the current strategy needs to be extended to further enhance the inter-cellular charge transport at significantly longer length scales. Thanks to their nanoscale structures and electrochemical activities, nanomaterials can be seamlessly integrated into existing EET pathways as conduits to electrically connect neighbouring bacteria to form a hybrid conductive network. This enables the linkage of electrode and distant bacteria, even the whole biofilm, to reach maximum EET efficiency.

For example, Zhang et al. have doped a biofilm on MFC anode with multiwall carbon nanotube (MWCNT) to increase its EET efficiency, thus improving the power generation.[76] Compared with natural biofilms, the MWCNT-doped biofilm has boosted current density (46.2%), power density (58.8%), and coulombic efficiency (84.6%). These results suggest that nanomaterials doping presents itself as a promising strategy to facilitate the long-range electron transfer. To further improve the electrical coupling between EABs and inorganic "dopants", different strategies have been exploited to seamlessly integrate electroactive nanomaterials into bacteria networks. In particular, EABs are known for their capability to reduce a wide range of minerals through EET. As-formed biogenic/biomineralized nanomaterials are highly desirable as electrical conduits since they could naturally connect with the active redox centres of OMCs which are usually wrapped by non-conductive peptide chain, thus remaining inaccessible during conventional physical mixing processes.[77] Other considerations for ideal nanomaterial conduits include: (i) reasonably good electrical conductivity so that there is no/little barrier for electron transfer through the nanoparticle itself and at nanoparticle/electrode interface; (ii) appropriate electrochemical potential so that the nanoparticle will act as mediators instead of being terminal electron acceptor; and (iii) good biocompatibility. Combing all these factors, iron minerals stand out as the perfect materials system and have recently been extensively investigated for facilitating EET at network levels.

Nakamura et al. have reported enhanced EET in *Shewanella loihica* PV-4 biofilm through doping the biofilm with n-type α-Fe_2O_3 nanoparticles.[78] According to the current measurements, after completely embedding α-Fe_2O_3 nanoparticles into PV-4 networks, the EET current increases 50 times as compared with that of the undoped control (Fig. 10). Also, the CV characterization clearly presents a 300 time increase of peak current at OMCs redox potential. These results suggest that the α-Fe_2O_3 nanoparticles can inter-connect the electron transfer pathways in the bacterial network, thus promoting long-range EET processes and enhancing the overall EET efficiency. Additionally, due to the unique photosensitive property of α-Fe_2O_3, the EET efficiency in this system

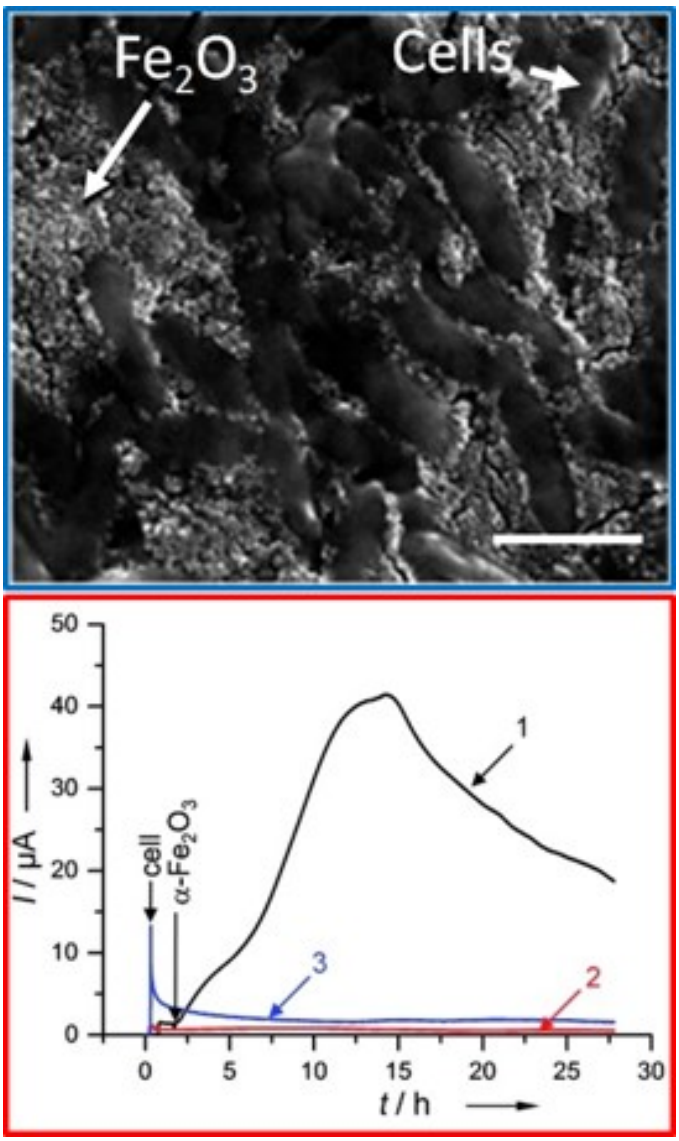

Fig. 10 Long range EET in α-Fe_2O_3 nanoparticle/bacteria hybrid network. (a) SEM image of the embed α-Fe_2O_3 nanoparticles in the bacteria network. Scale bar, 2 μm; (b) I-t curves in the presence (trace 1), absence (trace 2) of α-Fe_2O_3 nanoparticle and presence of Fe^{3+} (trace 3). Reprinted with permission from ref. 78. Copyright 2009 WILEY-VCH Verlag

can be further improved by diminishing the electron transfer energy barrier between the *Shewanella* OMCs and α-Fe_2O_3 through light illuminations.

Shewanella can also reduce both elemental sulfur and subsequently ferric iron to produce nanoscale mineral crusts with semiconductor-like properties through biomineralization. These crusts are directly coupled with the bacteria's electron transfer pathways, moderating long-range electron transfer from a few bacteria to external solid electron acceptors.[79,80] Jiang et al. have investigated the detailed mechanism of nanoparticle facilitated EET in *Shewanella loihica* PV-4 where $FeCl_3$ and $Na_2S_2O_3$ are used as iron and sulfur precursors to produce FeS nanoparticles at cellular interfaces.[81] The generated FeS nanoparticles are intimately bound to the bacteria membranes and interconnect to form 10–20 μm sized cell/nanoparticle aggregates. (Fig. 11) In particular, EET current generation is synchronized with the direct contact between bacteria-FeS. aggregates and electrode which indicates that FeS-EAB composites can perform the direct EET at bacteria/electrode interface. Moreover, the maximum current collected from definite number of bacteria/FeS aggregates (limited by the microscale open window) is about 500pA which is 3 to 4 order of magnitude higher than the reported values generated from single *Shewanella* or *Geobacter* cells. The enhancement in EET current suggests that FeS nanoparticles can facilitate the long range EET by constructing an electrically connected, three-dimensional cell network from bottom-up. Similarly, other biogenic nanomaterials such as Au and Pd nanoparticles as well as graphene oxide have also been used to facilitate EET in bacterial networks.[82–85]

In summary, this section provides an overview of diverse nanomaterial-enabled strategies to facilitate the bacteria EET. Beyond conventional strategies that only enhance the EET efficiencies by reducing electrode impedance, recent advances in the engineering of nanomaterial-bacteria interactions enable the rational design of effective EET pathways from bottom-up strategies. Nanomaterials offer superb electrical properties and tunability to reconcile the mismatches between bacteria and electrodes. The bio-enabled synthetic process further allows for the seamless integration of nanomaterials into existing charge transport pathways to promote EET at network levels. More recently, several studies demonstrate the potential of nanotechnologies in regulating biosynthesis of extracellular conductive materials. For example, when cultured on vertical silicon nanowire arrays, *Sporomusa ovata* can form filamentous cells that align parallel to nanowires with increasing ionic concentrations.[86] Hsu et al. create core/shell type bacteria "cables" in which the microenvironment and cell-cell interaction can be rationally controlled. This platform enables precise modulation of the structural (from membrane contact to

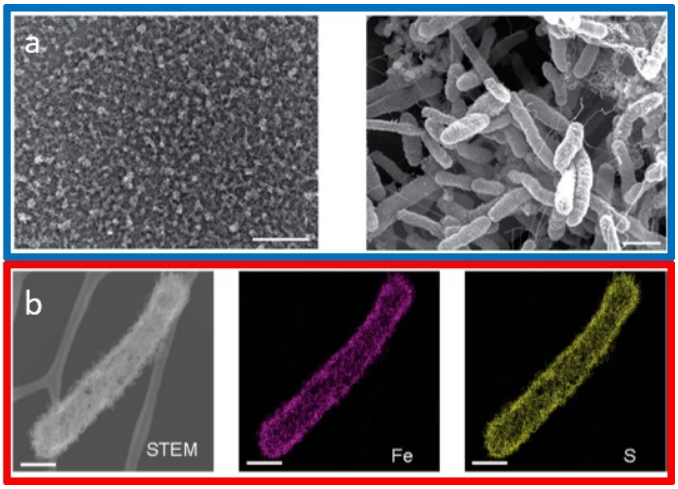

Fig. 11 Biogenic FeS nanoparticles enhance EET. (a) SEM image of FeS/bacteria aggregate under low and high magnifications. Scale bars, 100 μm (left) and 1 μm (right) (b) Bright-field STEM image and corresponding elemental mapping of a PV-4 cell coated with nanoparticles. Scale bar, 500 nm. Reprinted with permission from ref. 81. Copyright 2014 American Chemical Society

BNW connections) and electrical properties (from 2.5 to 162 $mS \cdot cm^{-1}$) of the one-dimensional conductive matrices generated by *Shewanella loihica* PV-4.[87] Moreover, Zhou et al. report that the introduction of TiO_2 nanoparticles during the culture of *Geobacter sulfurreducens* PCA can promote BNW formation, and the 2.7-fold increase in PilA protein expression can be directly translated to the improved EET.[88] Overall, these studies provide valuable insights into the rational design and production of biosynthetic electroactive materials which pave the way for their future bioelectronic applications. Based on these progresses, future developments in nanomaterial-bacteria hybrid systems are expected to elevate EET efficiencies to a completely new level, which will open up ample possibilities in the bioenergetic, bioelectronic, and other related research areas.

Conclusions and Future Outlooks

To summarize, nanotechnology-enabled platforms have been shown to allow for the rational customization of bacterial EET processes from bottom-up. These platforms have enabled researchers to precisely interrogate EET from single bacterium to network levels, providing critical insights into the fundamental mechanisms of EET that are difficult to achieve via population-level experiments. Furthermore, the rational design and integration of functional nanomaterials into the bacterial EET pathways can mediate the charge transport at both EAB/electrode and EAB/EAB interfaces, thus significantly enhancing the EET efficiency across multiple length scales. These efforts are advancing the understanding of energy metabolism and electron transfer in biological systems. Furthermore, the bacterium-nanomaterial hybrid systems allow seamless electrical contacts and matching energy levels at both bacterium-electrode and bacterium-bacterium interfaces. These strategies significantly improve the EET efficiencies, which lead to 40% to 200% increases in power generation from that of traditional MFCs. However, some studies indicate that nanomaterials could introduce unfavorable impacts to EABs. Maurer-Jones et al. suggest that the gene expression of *Shewanella oneidensis* is changed after exposure to TiO_2 nanoparticles. This effect not only significantly slows the biofilm development but also alters the EET of *S. oneidensis* toward the mediator (flavin) driven process.[89] More generally, several nanomaterials, such as carbon nanotube and (small, <10 nm) gold nanoparticles, are known to be cytotoxic.[90] Systematic studies of the influence of these nanomaterials to EAB physiology will be critical to provide important guidance in nanomaterial design and selection to optimize the EET efficiency without compromising the normal biological functions of EABs.

Moving forward, the fundamental EET elements, cyts, and their self-assembled materials stand out as a completely new category of biosynthetic electroactive materials with genetically encoded properties. The inherent conductivities of these materials can effectively mediate the electrical communications between biotic and abiotic systems. Their protein-based nature offers inherent biocompatibility as compared with traditional electronic materials such as metal, semiconductors and conductive polymers, making them uniquely qualified for many bio-interfacing applications. However, since the development of biofilm is uncontrolled, native cyt-based materials are intrinsically heterogeneous in terms of structures, compositions, and electrical properties. These complexities greatly challenge the structural design and fabrication processes, which demands the development of nano-manufacturing methods that allow precise control of the biosynthetic process to produce functional biomaterials with highly purity and rationally designed properties.

Overall, the integration of nanotechnology with biological systems offers tremendous opportunities in tackling both the fundamentals and applications of EET. Future research is expected to broaden the spectrum of introduced nanomaterials to better interpret, interrogate, and engineer these EET processes. These endeavours are opening doors for ample possibilities by bridging the gap between biological and artificial electronic systems, thus eventually transforming the way we communicate with biological systems.

Conflicts of interest

There are no conflicts to declare

Acknowledgements

The authors acknowledge the support from National Science Foundation (NSF DMR-1652095), NSERC Postdoctoral Fellowships Program (PDF-487877-2016) and Tufts Summer Scholars Program.

Notes and references

1 H. B. Gray and J. R. Winkler, *Annu. Rev. Biochem.*, 1996, **65**, 537–561.

2 A. Kumar, L. H.-H. Hsu, P. Kavanagh, F. Barrière, P. N. L. Lens, L. Lapinsonnière, J. H. Lienhard V, U. Schröder, X. Jiang and D. Leech, *Nat. Rev. Chem.*, 2017, **1**, 24.

3 B. E. Logan, B. Hamelers, R. Rozendal, U. Schröder, J. Keller, S. Freguia, P. Aelterman, W. Verstraete and K. Rabaey, *Environ. Sci. Technol.*, 2006, **40**, 5181–5192.

4 J. R. Kim, Y. E. Song, G. Munussami, C. Kim and B. H. Jeon, *Geosystem Eng.*, 2015, **18**, 173–180.

5 G. Biological and D. R. Lovley, *MBio*, 2017, **8**, e00695-17.

6 M. A. Lebedev and M. A. L. Nicolelis, *Trends Neurosci.*, 2006, **29**, 536–546.

7 L. F. Nicolas-Alonso and J. Gomez-Gil, *Sensors*, 2012, **12**, 1211–1279.

8 F. J. H. Hol and C. Dekker, *Science*, 2014, **346**, 1251821–1251821.

9 M. E. Hernandez, A. Kappler and D. K. Newman, *Appl. Environ. Microbiol.*, 2004, **70**, 921–928.

10 E. Marsili, D. B. Baron, I. D. Shikhare, D. Coursolle, J. a Gralnick and D. R. Bond, *Proc. Natl. Acad. Sci. U. S. A.*,

2008, **105**, 3968–3973.

11 D. K. Newman and R. Kolter, *Nature*, 2000, **405**, 94–7.

12 L. Shi, T. C. Squier, J. M. Zachara and J. K. Fredrickson, *Mol. Microbiol.*, 2007, **65**, 12–20.

13 L. Shi, H. Dong, G. Reguera, H. Beyenal, A. Lu, J. Liu, H.-Q. Yu and J. K. Fredrickson, *Nat. Rev. Microbiol.*, 2016, **14**, 651–662.

14 H. Richter, K. P. Nevin, H. Jia, D. A. Lowy, D. R. Lovley and M. Tender, *Energy Environ. Sci.*, 2009, **2**, 506.

15 Y. A. Gorby, S. Yanina, J. S. McLean, K. M. Rosso, D. Moyles, A. Dohnalkova, T. J. Beveridge, I. S. Chang, B. H. Kim, K. S. Kim, D. E. Culley, S. B. Reed, M. F. Romine, D. A. Saffarini, E. A. Hill, L. Shi, D. A. Elias, D. W. Kennedy, G. Pinchuk, K. Watanabe, S. Ishii, B. Logan, K. H. Nealson and J. K. Fredrickson, *Proc. Natl. Acad. Sci. U. S. A.*, 2006, **103**, 11358–11363.

16 S. Pirbadian, S. E. Barchinger, K. M. Leung, H. S. Byun, Y. Jangir, R. A. Bouhenni, S. B. Reed, M. F. Romine, D. A. Saffarini, L. Shi, Y. A. Gorby, J. H. Golbeck and M. Y. El-Naggar, *Proc. Natl. Acad. Sci. U. S. A.*, 2014, **111**, 12883–8.

17 G. Reguera, K. D. McCarthy, T. Mehta, J. S. Nicoll, M. T. Tuominen and D. R. Lovley, *Nature*, 2005, **435**, 1098–1101.

18 N. S. Malvankar and D. R. Lovley, *ChemSusChem*, 2012, **5**, 1039–1046.

19 N. S. Malvankar, M. Vargas, K. P. Nevin, A. E. Franks, C. Leang, B.-C. Kim, K. Inoue, T. Mester, S. F. Covalla, J. P. Johnson, V. M. Rotello, M. T. Tuominen and D. R. Lovley, *Nat. Nanotechnol.*, 2011, **6**, 573–579.

20 S. M. Strycharz-Glaven and L. M. Tender, *Energy Environ. Sci.*, 2012, **5**, 6250–6255.

21 N. S. Malvankar, M. T. Tuominen and D. R. Lovley, *Energy Environ. Sci.*, 2012, **5**, 6247–49.

22 S. M. Strycharz-Glaven, R. M. Snider, A. Guiseppi-Elie and M. Tender, *Energy Environ. Sci.*, 2011, **4**, 4366.

23 D. Coursolle, D. B. Baron, D. R. Bond and J. A. Gralnick, *J. Bacteriol.*, 2010, **192**, 467–474.

24 K. P. Nevin, B. C. Kim, R. H. Glaven, J. P. Johnson, T. L. Woodward, B. A. Methé, R. J. Didonato, S. F. Covalla, A. E. Franks, A. Liu and D. R. Lovley, PLoS One, 2009, **4**, e5628.

25 Y. Yang, M. Xu, J. Guo and G. Sun, *Process Biochem.*, 2012, **47**, 1707–1714.

26 M. Breuer, K. M. Rosso, J. Blumberger and J. N. Butt, *J. R. Soc. Interface*, 2015, **12**, 20141117.

27 D. R. Bond, S. M. Strycharz-Glaven, L. M. Tender and C. I. Torres, *ChemSusChem*, 2012, **5**, 1099–1105.

28 A. A. Carmona-Martinez, F. Harnisch, L. A. Fitzgerald, J. C. Biffinger, B. R. Ringeisen and U. Schröder, *Bioelectrochemistry*, 2011, **81**, 74–80.

29 Z. He and F. Mansfeld, *Energy Environ. Sci.*, 2009, **2**, 215–219.

30 B. E. Logan, *Microbial Fuel Cells*, John Wiley & Sons, Inc., 1st edn., 2008.

31 D. Das, *Microbial Fuel Cell-A Bioelectrochemical System that Converts Waste to Watts*, Springer International Publishing, 1st edn., 2018.

32 M. Grattieri, K. Hasan and S. D. Minteer, *ChemElectroChem*, 2017, **4**, 834–842.

33 H. Wang and Z. J. Ren, *Biotechnol. Adv.*, 2013, **31**, 1796–1807.

34 A. P. Borole, G. Reguera, B. Ringeisen, Z.-W. Wang, Y. Feng and B. H. Kim, *Energy Environ. Sci.*, 2011, **4**, 4813.

35 S. Choi, *Biosens. Bioelectron.*, 2015, **69**, 8–25.

36 D. R. Lovley, *Curr. Opin. Electrochem.*, 2017, **4**, 190–198.

37 G. Reguera, K. P. Nevin, J. S. Nicoll, S. F. Covalla, T. L. Woodard and D. R. Lovley, *Appl. Environ. Microbiol.*, 2006, **72**, 7345–7348.

38 M. Y. El-Naggar, G. Wanger, K. M. Leung, T. D. Yuzvinsky, G. Southam, J. Yang, W. M. Lau, K. H. Nealson and Y. A. Gorby, *Proc. Natl. Acad. Sci.*, 2010, **107**, 18127–18131.

39 R. Y. Adhikari, N. S. Malvankar, M. T. Tuominen and D. R. Lovley, *RSC Adv.*, 2016, **6**, 8354–8357.

40 B. F. Brehm-Stecher and E. A. Johnson, *Microbiol. Mol. Biol. Rev.*, 2004, **68**, 538–559.

41 S. V Avery, *Nat. Rev. Microbiol.*, 2006, **4**, 577.

42 X. Jiang, J. Hu, E. R. Petersen, L. a Fitzgerald, C. S. Jackan, A. M. Lieber, B. R. Ringeisen, C. M. Lieber and J. C. Biffinger, *Nat. Commun.*, 2013, **4**, 2751.

43 H. Liu, G. J. Newton, R. Nakamura, K. Hashimoto and S. Nakanishi, *Angew. Chemie*, 2010, **122**, 6746–6749.

44 X. Xie, C. Criddle and Y. Cui, *Energy Environ. Sci.*, 2015, **8**, 3418–3441.

45 X. Jiang, J. Hu, L. A. Fitzgerald, J. C. Biffinger, P. Xie, B. R. Ringeisen and C. M. Lieber, *Proc. Natl. Acad. Sci.*, 2010, **107**, 16806–16810.

46 R. M. Snider, S. M. Strycharz-Glaven, S. D. Tsoi, J. S. Erickson and L. M. Tender, *Proc. Natl. Acad. Sci.*, 2012, **109**, 15467–15472.

47 M. Ding, H. Y. Shiu, S. L. Li, C. K. Lee, G. Wang, H. Wu, N. O. Weiss, T. D. Young, P. S. Weiss, G. C. L. Wong, K. H. Nealson, Y. Huang and X. Duan, *ACS Nano*, 2016, **10**, 9919–9926.

48 P. S. Bonanni, D. F. Bradley, G. D. Schrott and J. P. Busalmen, *ChemSusChem*, 2013, **6**, 711–720.

49 E. Katz and I. Willner, *Angew. Chemie - Int. Ed.*, 2004, **43**, 6042–6108.

50 Y. Xiao, F. Patolsky, E. Katz, J. F. Hainfeld and I. Willner, Science, 2003, **299**, 1877-1881.

51 F. Patolsky, Y. Weizmann and I. Willner, *Angew. Chemie - Int. Ed.*, 2004, **43**, 2113–2117.

52 J. J. Gooding, R. Wibowo, J. Liu, W. Yang, D. Losic, S. Orbons, F. J. Mearns, J. G. Shapter and D. B. Hibbert, *J. Am. Chem. Soc.*, 2003, **125**, 9006–9007.

53 V. Pardo-Yissar, E. Katz, J. Wasserman and I. Willner, *J. Am. Chem. Soc.*, 2003, **125**, 622–623.

54 X. Xie, L. Hu, M. Pasta, G. F. Wells, D. Kong, C. S. Criddle and Y. Cui, *Nano Lett.*, 2011, **11**, 291–296.

55 X. W. Liu, J. J. Chen, Y. X. Huang, X. F. Sun, G. P. Sheng, D. B. Li, L. Xiong, Y. Y. Zhang, F. Zhao and H. Q. Yu, *Sci. Rep.*, 2014, **4**, 1–7.

56 G. C. Zhao, Z. Z. Yin, L. Zhang and X. W. Wei, *Electrochem. commun.*, 2005, **7**, 256–260.

57 X. Xie, M. Ye, L. Hu, N. Liu, J. R. McDonough, W. Chen, H. N. Alshareef, C. S. Criddle and Y. Cui, *Energy Environ. Sci.*, 2012, **5**, 5265–5270.

58 V. Flexer, J. Chen, B. C. Donose, P. Sherrell, G. G. Wallace and J. Keller, *Energy Environ. Sci.*, 2013, **6**, 1291.

59 H. Yuan and Z. He, *Nanoscale*, 2015, **7**, 7022–7029.

60 C. e. Zhao, J. Wu, Y. Ding, V. B. Wang, Y. Zhang, S. Kjelleberg, J. S. C. Loo, B. Cao and Q. Zhang, *ChemElectroChem*, 2015, **2**, 654–658.

61 C. Ding, H. Liu, Y. Zhu, M. Wan and L. Jiang, *Energy Environ. Sci.*, 2012, **5**, 8517.

62 C. Ding, H. Liu, M. Lv, T. Zhao, Y. Zhu and L. Jiang, *Nanoscale*, 2014, **6**, 7866.

63 C. E. Zhao, J. Wu, S. Kjelleberg, J. S. C. Loo and Q. Zhang, *Small*, 2015, **11**, 3440–3443.

64 F. A. Z. a. Alatraktchi, Y. Zhang and I. Angelidaki, *Appl. Energy*, 2014, **116**, 216–222.

65 Y. Fan, S. Xu, R. Schaller, J. Jiao, F. Chaplen and H. Liu, *Biosens. Bioelectron.*, 2011, **26**, 1908–1912.

66 X. Jia, Z. He, X. Zhang and X. Tian, *Synth. Met.*, 2016, **215**, 170–175.

67 X.-B. Gong, S.-J. You, Y. Yuan, J.-N. Zhang, K. Sun and N.-Q. Ren, *ChemElectroChem*, 2015, **2**, 1307–1313.

68 Y. Qiao, X. S. Wu and C. M. Li, *J. Power Sources*, 2014, **266**, 226–231.

69 R. Bian, Y. Jiang, Y. Wang, J. Sun, J. Hu, L. Jiang and H. Liu, Adv. Funct. Mater. 2018, **28**, 1707408.

70 J. Ji, Y. Jia, W. Wu, L. Bai, L. Ge and Z. Gu, *Colloids Surfaces A Physicochem. Eng. Asp.*, 2011, **390**, 56–61.

71 X. Peng, H. Yu, X. Wang, N. Gao, L. Geng and L. Ai, *J. Power Sources*, 2013, **223**, 94–99.

72 X. Peng, H. Yu, X. Wang, Q. Zhou, S. Zhang, L. Geng, J. Sun and Z. Cai, *Bioresour. Technol.*, 2012, **121**, 450–453.

73 F. Qian, H. Wang, Y. Ling, G. Wang, M. P. Thelen and Y. Li, *Nano Lett.*, 2014, **14**, 3688–3693.

74 H. Nie, T. Zhang, M. Cui, H. Lu, D. R. Lovley and T. P. Russell, *Phys. Chem. Chem. Phys.*, 2013, **15**, 14290–14294.

75 T. Zhang, H. Nie, T. S. Bain, H. Lu, M. Cui, O. L. Snoeyenbos-West, A. E. Franks, K. P. Nevin, T. P. Russell and D. R. Lovley, *Energy Environ. Sci.*, 2013, **6**, 217–224.

76 P. Zhang, J. Liu, Y. Qu, J. Zhang, Y. Zhong and Y. Feng, *J. Power Sources*, 2017, **361**, 318–325.

77 B. H. Kim, H. J. Kim, M. S. Hyun and D. H. Park, *J. Microbiol. Biotechnol.*, 1999, **9**, 127–131.

78 R. Nakamura, F. Kai, A. Okamoto, G. J. Newton and K. Hashimoto, *Angew. Chemie - Int. Ed.*, 2009, **48**, 508–511.

79 T. M. Flynn, E. J. O. Loughlin, B. Mishra, T. J. Dichristina and K. M. Kemner, *Science*, 2014, **344**, 1039–1043.

80 R. Nakamura, A. Okamoto, N. Tajima, G. J. Newton, F. Kai, T. Takashima and K. Hashimoto, *ChemBioChem*, 2010, **11**, 643–645.

81 X. Jiang, J. Hu, A. M. Lieber, C. S. Jackan, J. C. Biffinger, L. A. Fitzgerald, B. R. Ringeisen and C. M. Lieber, *Nano Lett.*, 2014, **14**, 6737–6742.

82 R. Wu, L. Cui, L. Chen, C. Wang, C. Cao, G. Sheng, H. Yu and F. Zhao, *Sci. Rep.*, 2013, **3**, 1–7.

83 X. Wu, F. Zhao, N. Rahunen, J. R. Varcoe, C. Avignone-Rossa, A. E. Thumser and R. C. T. Slade, *Angew. Chemie - Int. Ed.*, 2011, **50**, 427–430.

84 Y. Yuan, S. Zhou, B. Zhao, L. Zhuang and Y. Wang, *Bioresour. Technol.*, 2012, **116**, 453–458.

85 S. Kato, R. Nakamura, F. Kai, K. Watanabe and K. Hashimoto, *Environ. Microbiol.*, 2010, **12**, 3114–3123.

86 K. K. Sakimoto, C. Liu, J. Lim and P. Yang, *Nano Lett.*, 2014, **14**, 5471–5476.

87 L. H. H. Hsu, D. Pu, Y. Zhang and X. Jiang, *Nano Lett.* ***DOI:*** *10.1021/acs.nanolett.8b01908*

88 S. Zhou, J. Tang, Y. Yuan, G. Yang and B. Xing, *Environ. Sci. Technol. Lett.*, ***DOI****:10.1021/acs.estlett.8b00275.*

89 M. A. Maurer-Jones, I. L. Gunsolus, B. M. Meyer, C. J. Christenson and C. L. Haynes, *Anal. Chem.*, 2013, **85**, 5810–5818.

90 A. Kunzmann, B. Andersson, T. Thurnherr, H. Krug, A. Scheynius and B. Fadeel, *Biochim. Biophys. Acta - Gen. Subj.*, 2011, **1810**, 361–373.

91 X. Xie, G. Yu, N. Liu, Z. Bao, C. S. Criddle and Y. Cui, Energy Environ. Sci., 2012, **5**, 6862–6866